Journal of Structural Geology 56 (2013) 34–44

Contents lists available at ScienceDirect

Journal of Structural Geology

journal homepage: www.elsevier.com/locate/jsg

Weathering history of an exposed bedrock fault surface interpreted from its topography

Zhanyu Wei, Honglin He*, Feng shi

Key Laboratory of Active Tectonics and Volcano, Institute of Geology, China Earthquake Administration, Beijing 100029, China

ARTICLE INFO

Article history:
Received 19 January 2013
Received in revised form
11 August 2013
Accepted 22 August 2013
Available online 30 August 2013

Keywords:
Bedrock fault surface
Weathering
Roughness
Faulting

ABSTRACT

Morphologic features of bedrock fault scarps are underutilized in studying faulting and weathering history, partly because of a lack of accurate quantitative parameters for topography. The study employs ground-based LiDAR to measure five patches at different levels on the same fault surface and then calculates roughness in the form of power spectral density in directions parallel and perpendicular to the slip. The power spectral density and spatial frequency typically follow a power law for each fault patch, showing approximately linear relationships in a log–log plot. However, due to additional power introduced by weathering, all spectral curves, especially those parallel to the slip, can be divided into two segments, lower-frequency (wavelengths of several centimeters – several meters) and higher-frequency (wavelengths of several centimeters and below) domains. This shows that the topographic features at different spatial scales are dominated by different mechanical processes: faulting abrasion in the lower-frequency domain and the weathering process in the higher-frequency domain. Moreover, we develop two parameters to quantify the degree of weathering of a fault outcrop, which is significant to describe the evolution of the fault-scarp and infer the date of faulting under calibration.

1. Introduction

A fault scarp is an important specific tectonic landform caused by faulting, either in unconsolidated sediments or in bedrock. The morphology of the fault scarp in unconsolidated sediments could be used to establish faulting history by a diffusion model (Andrews and Hanks, 1985; Nash, 1986; Arrowsmith et al., 1998), whereas a bedrock fault scarp does not evolve in the same predictable, time-dependent fashion as an equivalent scarp in unconsolidated sediments. As a result, a bedrock scarp is not considered a sensitive indicator of the timing and magnitude of past faulting events (Mayer, 1984; Stewart, 1993). However, other researchers have reported paleoseismological implications of bedrock fault scarps and described their morphologies in an attempt to extract useful information concerning earthquake recurrence intervals. For example, Wallace (1984) and Stewart (1996) delimited the slip increment of every faulting event by identifying different parallel weathered bands on exposed fault planes. Giaccio et al. (2002) made use of image processing and roughness analysis of an exposed bedrock fault surface as a paleoseismological analysis tool in the Campo Felic fault. In the last several years, bedrock fault scarps have become an attractive alternative for paleoseismological studies because the exposure duration of a bedrock fault scarp can be determined directly by methods based on the accumulation of cosmogenic nuclides (Zreda and Noller, 1998; Benedetti et al., 2000; Mitchell et al., 2001). The dating result of cosmogenic nuclides close to the bedrock fault surface may, however, have an ambiguous interpretation of faulting history due to interference from the surroundings and the weathering of the bedrock fault surface, and the ambiguity may be identified through the combination of a micro-morphologic analysis of the exposed fault scarps (Mitchell et al., 2001).

For some time geologists have noted that the surface of rocks vary systematically in their weathering characteristics, and have developed methods to estimate exposure time based on progressive and time-dependent changes of rock surface morphology (Birkeland and Noller, 2000), such as the statistics of erosion and lichen pitting (Burke and Birkeland, 1979; Smirrnova and Nikonov, 1990; Ren and Li, 1993; Noller and Locke, 2000; Ehlmann et al., 2008). These methods are simple and inexpensive. However,

* Corresponding author. Tel.: +86 10 62009215.
E-mail addresses: weizhanyu@gmail.com (Z. Wei), honglinhe123@vip.sina.com, honglin@ies.ac.cn (H. He), skywazy@126.com (F. shi).

0191-8141/$ – see front matter © 2013 Elsevier Ltd. All rights reserved.
http://dx.doi.org/10.1016/j.jsg.2013.08.008

because it is labor intensive, only a few samples were reported for each surface, and the results are vulnerable to the operators' experience and subjectivity. Progressive surface weathering often leads to increased surface roughness; the more eroded by weathering the topography is, the rougher the surface. Surface roughness could be an indicator of the degree of weathering of the rock surface (McCarroll and Nesje, 1996).

The aim of this research is to quantify the degree of weathering of a bedrock fault surface, which is meaningful in building a relationship between exposure time and degree of weathering. We chose a limestone fault surface near Beijing and measured its topography utilizing ground-based LiDAR (Light Detection And Ranging), which is popular for measuring the topography of fault surfaces in the field (Sagy et al., 2007; Brodsky et al., 2010; Wei et al., 2010). After reviewing the methodology, we presented roughness measurements in the form of power spectral density in directions parallel and perpendicular to the slip. A new approach for quantifying the progressive degree of weathering of a bedrock fault surface based on surface roughness is proposed, and the result shows that the roughness in a high frequency band depends on the exposure time of the fault surface. Finally, we discuss how this new approach could be used to evaluate the exposure time or even the faulting time of a bedrock fault surface.

2. Scanned fault scarp and its geologic site

Nearly adjacent to the Tibetan Plateau, the Ordos block bridges the intensively uplifted Plateau and the disassembled old North China Craton (Jolivet et al., 2001; Wang et al., 2011). Surrounding the block, four faulted-depression basin belts develop: Shanxi Faulted-depression Basin Belt (SFB) in east, Yinchuan-Jilantai Faulted-depression Basin Belt (YFB) in west, Hetao Faulted-depression Basin Belt (HFB) in north and Weihe Faulted-depression Basin Belt (WFB) in south (Xu and Ma, 1992; Deng et al., 1999) (Fig. 1a). In these faulted-depression basins, a lot of fault scarps crop out.

The Shizhuang fault, our target fault is an active fault in Late Pleistocenc-Holocene era (Ran et al., 1992), and crosses the Yanhuai basin in the direction of 300°–320° and dips northeastward at 60°–80° (Fig. 1b). The Huailai basin located northwest of Beijing, is one of the faulted-depression basins in the Shanxi Faulted-depression Basin Belt (Fig. 1a). The scanned fault scarp crops out

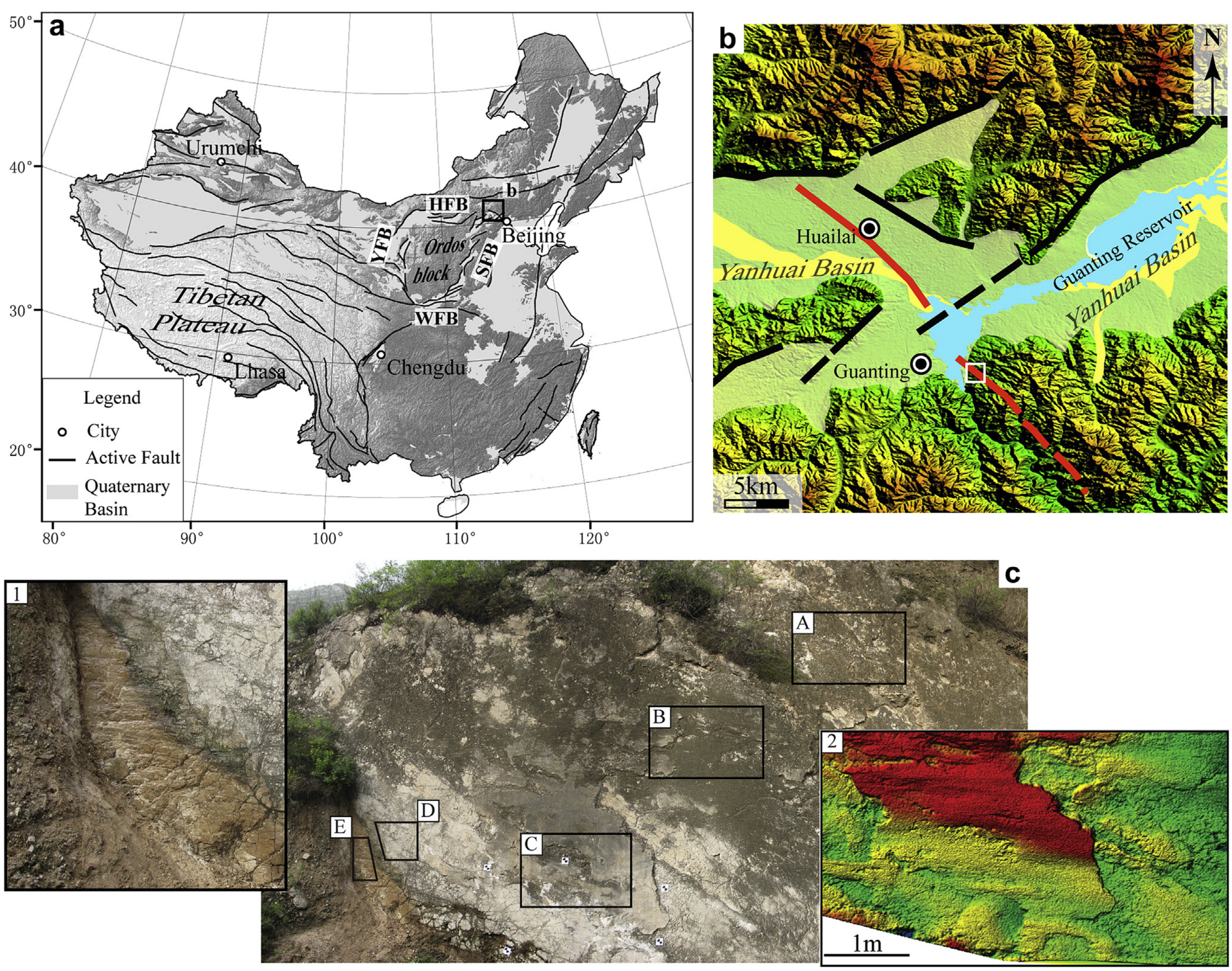

Fig. 1. Sketch map on tectonics of China and fault surface pictures. (a) Main active fault distribution of China (modified from Deng, 2007), black lines indicate active faults; black rectangle shows the location of (b); (b) Topographical map and fault distribution in Yanhuai Basin. Red lines indicate Shizhuang Fault and black lines indicate other faults; the base map is from ASTER Global DEM data; white rectangle shows the location of (c); (c) Photographs of the target fault surface. Five black boxes, labeled A, B, C, D and E, show the locations of the scanned surface patches. Inset 1 is the enlarged view of excavated patch E; Inset 2 is the LiDAR image of the target fault surface in color-scale produced by – one million scanning points with 5-mm-spacing on average. (For interpretation of the references to color in this figure legend, the reader is referred to the web version of this article.)